Published in final edited form as:
J Comp Neurol. 2012 April 1; 520(5): 1047–1061. doi:10.1002/cne.22769.

Pre-Bötzinger Complex Receives Glutamatergic Innervation From Galaninergic and Other Retrotrapezoid Nucleus Neurons

Genrieta Bochorishvili, **Ruth L. Stornetta**, **Melissa B. Coates**, and **Patrice G. Guyenet***
Department of Pharmacology, University of Virginia, Charlottesville, Virginia 22908

Abstract

The retrotrapezoid nucleus (RTN) contains CO_2-responsive neurons that regulate breathing frequency and amplitude. These neurons (RTN-Phox2b neurons) contain the transcription factor Phox2b, vesicular glutamate transporter 2 (VGLUT2) mRNA, and a subset contains preprogalanin mRNA. We wished to determine whether the terminals of RTN-Phox2b neurons contain galanin and VGLUT2 proteins, to identify the specific projections of the galaninergic subset, to test whether RTN-Phox2b neurons contact neurons in the pre-Bötzinger complex, and to identify the ultrastructure of these synapses. The axonal projections of RTN-Phox2b neurons were traced by using biotinylated dextran amine (BDA), and many BDA-ir boutons were found to contain galanin immunoreactivity. RTN galaninergic neurons had ipsilateral projections that were identical with those of this nucleus at large: the ventral respiratory column, the caudolateral nucleus of the solitary tract, and the pontine Köliker-Fuse, intertrigeminal region, and lateral parabrachial nucleus. For ultrastructural studies, RTN-Phox2b neurons (galaninergic and others) were transfected with a lentiviral vector that expresses mCherry almost exclusively in Phox2b-ir neurons. After spinal cord injections of a catecholamine neuron-selective toxin, there was a depletion of C1 neurons in the RTN area; thus it was determined that the mCherry-positive terminals located in the pre-Bötzinger complex originated almost exclusively from the RTN-Phox2b (non-C1) neurons. These terminals were generally VGLUT2-immunoreactive and formed numerous close appositions with neurokinin-1 receptor-ir pre-Bötzinger complex neurons. Their boutons (n = 48) formed asymmetric synapses filled with small clear vesicles. In summary, RTN-Phox2b neurons, including the galaninergic subset, selectively innervate the respiratory pattern generator plus a portion of the dorsolateral pons. RTN-Phox2b neurons establish classic excitatory glutamatergic synapses with pre-Bötzinger complex neurons presumed to generate the respiratory rhythm.

INDEXING TERMS

central respiratory chemoreception; respiratory network; brainstem

The non-catecholaminergic, non-cholinergic Phox2b-expressing neurons of the retrotrapezoid nucleus (hereafter called the RTN-Phox2b neurons) are critical for central respiratory chemoreception, the process by which an increase in brain PCO_2 stimulates breathing (Pattyn et al., 1997; Takakura et al., 2008; Marina et al., 2010; Goridis and Brunet, 2010; Guyenet et al., 2010b). Their strong response to increases in PCO_2 in vivo probably relies on at least four factors: their intrinsic acid sensitivity, a paracrine regulation by surrounding astrocytes, inputs from peripheral chemoreceptors, and inputs from other CO_2-

*CORRESPONDENCE TO: Patrice G. Guyenet, Ph. D., University of Virginia Health System, P.O. Box 800735, 1300 Jefferson Park Avenue, Charlottesville, VA 22908-0735. pgg@virginia.edu.

sensitive CNS neurons (Nattie and Li, 2008; Gourine et al., 2010; Guyenet et al., 2010b). The RTN-Phox2b neurons are probably glutamatergic because they contain the mRNA that encodes vesicular glutamate transporter 2 (VGLUT2), and breathing is strongly activated when these neurons are stimulated (Takamori et al., 2001; Mulkey et al., 2004; Abbott et al., 2009c; Guyenet et al., 2010b). However, the projections of the RTN-Phox2b neurons are not well described, and there is no information as to whether these neurons make conventional synapses. Finally, a large subset of RTN-Phox2b neurons expresses preprogalanin mRNA (Stornetta et al., 2009), but the specific anatomical projections of these neurons are unknown.

We have previously generated a general overview of the axonal projections of the RTN-Phox2b neurons by using a lentiviral vector that expresses its transgene under the control of the artificial promoter PRSx8 (Abbott et al., 2009c). Given adequate precautions (titer and amount of vector injected), this method selectively tracks the projections of the ventrolateral medullary neurons that express Phox2b (Pattyn et al., 1997; Hwang et al., 2001; Abbott et al., 2009c). However, this cell population always includes C1 adrenergic neurons, the occasional A5 noradrenergic neuron, and a few cholinergic neurons (Card et al., 2006; Stornetta et al., 2006). Although the number of C1 and A5 neurons that express ChR2-mCherry after virus injection into the RTN region can be substantially reduced by administration of a catecholaminergic neuron-selective neurotoxin into the spinal cord, the C1 and A5 neurons are never completely eliminated (Schreihofer et al., 2000; Abbott et al., 2009c). Therefore, the PRSx8-ChR2-mCherry lentiviral method is not selective enough to identify the axonal projections of the RTN-Phox2b chemoreceptors with absolute certainty.

The first objective of the present study was to produce a more definitive map of the projections of RTN-Phox2b neurons that would be uncontaminated by processes from the C1 and other Phox2b-expressing neurons. We addressed this question by tracking the projections of the galaninergic subset of RTN-Phox2b neurons using a simple adaptation of the conventional biotinylated dextran amine (BDA) method. This approach takes advantage of the fact that the galaninergic RTN-Phox2b neurons are isolated from any other group of galaninergic neurons.

The remaining objectives of the study were to determine whether RTN-Phox2b neurons innervate the pre-Bötzinger complex, the region of the ventrolateral medulla that contains the core of the respiratory rhythm-generating circuitry (Smith et al., 1991; Feldman et al., 2003; Janczewski and Feldman, 2006; Smith et al., 2009). This region is noted for its concentration of neurons that express a very high level of neurokinin-1 receptors, most of which are respiratory neurons that regulate the breathing rate (Gray et al., 2001; Guyenet et al., 2002; Tan et al., 2008). We determined whether the RTN-Phox2b neurons make close appositions with neurons in this region and examined the ultrastructure of these synapses.

MATERIALS AND METHODS

Animal experiments were done in adult Sprague Dawley rats (250–350 g; Taconic; Germantown, NY). Procedures were in accordance with National Institutes of Health Animal Care and Use Committee Guidelines and were approved by the University of Virginia Animal care and Use Committee.

Surgery and tracer injections

All surgeries used standard aseptic methods in rats that were deeply anesthetized with a mixture of ketamine (75 mg/kg), xylazine (5 mg/kg), and acepromazine (1 mg/kg). Immediately after surgery and on the morning after, the rats received an antibiotic (ampicillin, 100 mg/kg, i.m.; American Pharmaceutical Partners, Schaumberg, IL) and an

analgesic (ketorolac tromethamine; 0.6 mg/kg, s.c.; Abbott Laboratories, North Chicago, IL). Animals were maintained for 4 weeks before they were used in immunohistochemical experiments.

BDA injections in normal rats (n = 10)—BDA (lysine-fixable, MW 10,000; 10% w/v in 10 mM phosphate buffer [PB], pH 7.4; Molecular Probes, Eugene, OR) was injected by iontophoresis (5-μA positive current for 5 seconds every 10 seconds for 10 minutes) into the caudal end of the left RTN as described in a prior publication (Rosin et al., 2006). Satisfactory BDA deposits were obtained in three rats, and only these cases are described in the Results section.

Lentiviral vector injections in adrenergic neuron-depleted rats (n = 5)—Each rat first received bilateral injections of anti-dopamine-β-hydroxylase conjugated to saporin (anti-DβH-sap; Advanced Targeting Systems [San Diego, CA] diluted with sterile saline to 0.22 μg/μl) into the thoracic spinal cord (level T3; two injections per side; 100 nl per injection) to reduce the number of C1 adrenergic neurons with spinal projections. We then injected the RTN with a previously described lentiviral vector that expresses enhanced channelrhodopsin-2 fused with mCherry under the control of the artificial promoter PRSx8 (pLenti-PRSx8-hChR2 [H134]-mCherry-WPRE, henceforth abbreviated PRSx8-ChR2-mCherry; Abbott et al., 2009b).

The virus was produced by the University of North Carolina virus core and diluted to a final titer of 3.0×10^8 pfu/ml with sterile phosphate-buffered saline (PBS) before injection into the brain. At this concentration of the vector, the transgene, ChR2-mCherry, is selectively expressed by Phox2b-containing neurons that, in the rostral ventrolateral medulla, consist virtually exclusively of RTN chemoreceptive neurons and C1 adrenergic neurons (Abbott et al., 2009b, c; Kanbar et al., 2010). The lentivirus was delivered into the RTN by controlled pressure injections (60 psi; 3–8-ms pulses) using glass pipettes (tip diameter 25 μm) with resistance 6–12 MΩ. Two injections were made on the left side under electrophysiological guidance (total volume: 400 nl) by using antidromic activation of the facial motor neurons to determine the extent and location of the facial motor nucleus and thus the location of the RTN directly ventral and caudal to this nucleus (Abbott et al., 2009b, c; Kanbar et al., 2010).

Light microscopy (LM) histology—Twelve adult rats were deeply anesthetized and perfused transcardially with 500 U heparin and 100 ml PBS (pH 7.4), followed by freshly prepared 4% paraformaldehyde in 100 mM sodium PB (pH 7.4; Electron Microscopy Sciences, Fort Washington, PA). The brains were removed and stored in the perfusion fixative for 24–48 hours at 4°C. Series of coronal sections (30 μm) were cut on a vibrating microtome (Leica, Nussloch, Germany) at room temperature and stored in cryoprotectant solution at −20°C (20% glycerol, 30% ethylene glycol in 50 mM PB, pH 7.4).

All immunohistochemical procedures were performed in a one-in-six series of sections. All sections were initially rinsed in 0.1 M Tris-buffered saline pH 7.4 (TBS), blocked in 10% horse serum and 0.1% Triton X-100 (Sigma-Aldrich, St. Louis, MO) in TBS, and incubated for 24–72 hours at 4°C with primary antibody. Sections were then rinsed in TBS, incubated for 30–40 minutes in secondary antibodies, and then rinsed in TBS. Sections for transmitted LM were further reacted with colorization reagents as described below. All sections were mounted from 0.1 M PB onto glass slides, air-dried, dehydrated through a graded series of alcohols and xylenes, and covered with DPX (Sigma-Aldrich).

For revealing BDA-labeled neuronal processes originating in the RTN, sections were incubated in rabbit anti-galanin (1:1,000; Peninsula, San Carlos, CA) and mouse anti-tyrosine hydroxylase (TH; MAB318, 1:1,000; Millipore, Billerica, MA). BDA was revealed

with Alexa 488-tagged avidin (1:200; Invitrogen, Carlsbad, CA) in combination with either anti-mouse IgG-Cy3 (for TH, 1:200; Jackson ImmunoResearch, West Grove, PA) or anti-rabbit IgG-Cy3 (for galanin; 1:200, Jackson ImmunoResearch).

For identifying RTN-Phox2b neuronal processes with fluorescence microscopy, sections were incubated with rabbit anti-DsRed antibody to detect mCherry (1:500; Clontech, Mountain View, CA) in combination with either TH primary antibody (described above) or VGLUT2 primary antibody (guinea pig anti-VGLUT2, 1:2,000; Millipore). mCherry was revealed with anti-rabbit IgG-Cy3 (Jackson ImmunoResearch), and TH was revealed with anti-mouse IgG- Alexa 488 (1:200, Invitrogen) or VGLUT2 was revealed with anti-guinea pig IgG-Alexa 488 (1:200, Invitrogen).

For identifying RTN-Phox2b neuronal processes by transmitted LM, sections were processed sequentially with anti-DsRed (described above) and anti-neurokinin1 receptor (NK1R) primary antibodies (1:1,000; Sigma). Initially sections were incubated in anti-DsRed (1:500, Clontech). After 18 hours, sections were rinsed in TBS and then incubated in biotinylated donkey anti-rabbit IgG (1:100, Jackson ImmunoResearch), rinsed, and incubated in avidin-biotin peroxidase complex (ABC Elite, according to the manufacturer's instructions, Vector, Burlingame, CA). After rinsing in TBS, sections were incubated for 10 minutes with 0.02% diaminobenzidine (DAB; Sigma-Aldrich, St. Louis, MO) and 0.03% hydrogen peroxide in 0.1 M Tris buffer and 0.2% nickel ammonium sulfate to reveal mCherry processes in black. Sections were washed with multiple rinses in 0.1 M PB (pH 7.4). Sections were then incubated for 48 hours in rabbit polyclonal NK1R antibody (1:1,000, Sigma-Aldrich), rinsed in TBS, incubated in biotinylated donkey anti-rabbit IgG (1:200, Jackson ImmunoResearch), rinsed again, and incubated in ABC Elite (Vector; according to the manufacturer's instructions). After rinsing in TBS, sections were reacted for 6 minutes with 0.02% DAB and 0.03% hydrogen peroxide in 0.1 M Tris buffer to reveal NK1R neuronal membranes in brown.

All sections were observed by using a Zeiss Axioimager.Z1 and digitally photographed with a Zeiss MRc camera. The resulting TIFF files were imported into Adobe Photoshop (Version 7; Adobe Systems, Mountain View, CA). Output levels were adjusted to include all information-containing pixels. Balance and contrast were adjusted to reflect true rendering as much as possible. The red channel is represented as magenta in all material photographed with fluorescent tags. Some of the high-power images of fluorescent boutons were taken as z-stacks at 0.5–1-μm intervals and deconvoluted through 10 passes by using AutoDeblur software (Media Cybernetics, Bethesda). No other photo retouching was done. Figures were assembled and labeled by using Canvas software (Version 10; ACD Systems, Miami, FL).

Electron microscopy (EM) histology—Three adult rats injected 4 weeks prior with lentiviral vector injected into the RTN and antiDβH-sap toxin injected into the spinal cord were deeply anesthetized (see above) and perfused through the heart with the following solutions: 50 ml of a mixture of 3.78% acrolein (Electron Microscopy Sciences) and 2% paraformaldehyde in 0.1 M PB, pH 7.4, followed by 100 ml of 2% paraformaldehyde in PB. Brains were postfixed in 2% parafor-maldehyde for 2 hours. Sections were cut on a vibrating microtome at a thickness of 30 μm, treated with 1% sodium borohydride (Sigma-Aldrich) in PB for 30 minutes, rinsed in PB several times, rinsed in 0.1 M TBS, and incubated for 30 minutes in blocking solution of 1% bovine serum albumin and 0.04% Triton X-100 in TBS. Sections were incubated with anti-DsRed antibody to detect mCherry (1:500; rabbit anti-DsRed, Clontech).

After overnight incubation (14–18 hours, 4°C), tissue was rinsed in TBS, incubated for 30 minutes in biotinylated goat anti-rabbit secondary antibody (1:200; Jackson

ImmunoResearch), rinsed again, and incubated for 30 minutes in ABC Elite. After rinsing in TBS, sections were reacted for 6 minutes with 0.02% DAB and 0.03% hydrogen peroxide in TBS, followed by rinses in PB. Sections were then incubated for 1 hour in 1% osmium tetroxide (Electron Microscopy Sciences) in PB. The tissue was then dehydrated in ascending concentrations of ethanol (50%, 70%, 95%, 100%), followed by propylene oxide (Electron Microscopy Sciences) and then infiltrated with a 1:1 mixture of propylene oxide and Embed-812 embedding resin (Electron Microscopy Sciences). This mixture was subsequently replaced with pure resin for 2 hours. The sections were flat-embedded and heated for up to 48 hours at 60°C. Ultrathin sections (75–80 nm) from the pre-Bötzinger complex region of the ventrolateral medulla were collected on mesh grids and analyzed on a transmission electron microscope (JEOL 1230 with real-time digital imaging (2Kx2K); Peabody, MA).

Antibodies

The following antibodies were used:

1. Mouse anti-TH monoclonal antibody (MAB318; Millipore) was raised against tyrosine hydroxylase purified from PC12 cells and recognizes an epitope on the outside of the regulatory N-terminus of tyrosine hydroxylase. As reported by Millipore, this antibody recognizes a protein of approximately 59–63 kDa by Western blot and does not cross-react with dopamine-β-hydroxylase, phenylalanine hydroxylase, tryptophan hydroxylase, or phenyl ethanolamine-N-methyl transferase on Western blots of brain lysates. The labeling produced in the current study was seen in cell soma and dendrites as well as putative terminals, and the pattern of labeling was restricted to known catecholamine cell groups. The immunolabeling with TH observed in the present study was similar to that seen in many previous studies in our laboratory using identical methods (Kang et al., 2007; Takakura et al., 2008; Abbott et al., 2009b).

2. Rabbit anti-DsRed polyclonal antibody (Living Colors DsRed polyclonal antibody 632496; Clontech) was raised against DsRed-Express, a variant of *Dicosoma* sp. red fluorescent protein. It recognizes all the red fluorescent “fruit” protein variants including mCherry. No labeling was present in tissue without injections of the ChR2-mCherry lentivirus.

3. Rabbit anti-galanin polyclonal antibody (T-4334; Peninsula) was raised against a synthetic peptide (GWTLNSAGYLLGPHAIDNHRSFSDKHGLT; sequence from rat galanin) and cross-reacts with rat, human, and porcine galanin but not with secretin, vasoactive intestinal peptide (VIP), substance P, or neuropeptide Y (NPY; tested by radioimmunoassay as reported by the manufacturer). Preincubation of the antibody with the immunizing peptide blocks all immunolabeling (Landry et al., 2006).

4. Rabbit anti-NK1R polyclonal antibody (S8305; Sigma-Aldrich) was raised against a synthetic peptide (KTMTESSSFYS-NMLA) corresponding to the C-terminus of the rat substance P receptor (NK-1), which was conjugated to keyhole limpet hemocyanin. The antibody recognizes a single band of 45 kDa (corresponding to the NK1R protein) on Western blots of rat brain lysate. This labeling is specifically inhibited by the immunizing peptide (according to the manufacturer). Furthermore, there is no immunolabeling in sections of medulla and cervical spinal cord from mice in which the NK1R has been deleted ($NK1R^{-/-}$), whereas staining is present in sections from wild-type mice (Ptak et al., 2002). The immunolabeling observed in the present study was similar to that seen in previous studies in our laboratory using identical methods (Wang et al., 2003; Stornetta et al., 2003a).

5. Guinea pig anti-VGLUT2 antibody (AB2251; Millipore) was raised against a recombinant GST-tagged peptide (VQESAQDAYSYKDRDDYS) corresponding to the C-terminus of the rat VGLUT2 protein. The antibody recognizes a band of 56 kDa (corresponding to the VGLUT2 protein) on Western blots of rat brain lysate. Immunolabeling was absent when the primary antibody was first incubated with the immunogen. The immunolabeling observed in the present study was similar to that seen in a previous study in our laboratory using identical methods (Stornetta et al., 2003b).

RESULTS

Projections of RTN galaninergic neurons

Figure 1A reiterates our previous observation that the RTN contains a distinctive cluster of neurons that express preprogalanin mRNA (all material in Fig. 1 generated from a previous study [Stornetta et al., 2009]). As seen in Figure 1B, and of critical importance to the present study, this is the only galaninergic cell group identifiable at this level of the medulla oblongata. In the rat, the nearest groups of putative galaninergic neurons are at a considerable distance (nucleus of solitary tract caudal to area postrema, ventrolateral medulla, also caudal to area postrema level; results not illustrated). Figure 1B also reiterates the fact that the RTN galaninergic neurons are all Phox2b-positive (Stornetta et al., 2009). We also previously demonstrated that the Phox2b-containing neurons located within this brain region contain VGLUT2 mRNA and are therefore presumed to be glutamatergic (Stornetta et al., 2006). Galaninergic neurons are found throughout the rostrocaudal extent of the RTN both the marginal layer and dorsal cap (Stornetta et al., 2009).

In the present study, we determined the projections of the putatively galaninergic neurons of the RTN by injecting small amounts of the anterograde marker BDA in their midst (Fig. 2A, B) and subsequently mapping the location of axons and terminals that were immunoreactive for both BDA and galanin (Fig. 2C). In order to increase our chances of labeling galaninergic neurons, we deliberately targeted the caudal end of the RTN where the density of these neurons is greatest (Stornetta et al., 2009). The following describes three cases in which BDA was accurately targeted to the caudal portion of the RTN (Fig. 2B). There were a large number of BDA-positive galanin-immunoreactive (ir) terminals in all three cases. These terminals were detected exclusively within the following pontomedullary regions: ventrolateral medulla, caudal lateral nucleus of the solitary tract, intertrigeminal area, Kölliker-Fuse nucleus, and lateral parabrachial region (Fig. 3).

In all these regions, the vast majority of the galanin-ir terminals were BDA-negative. These terminals likely originated from the numerous galaninergic neurons located in the nucleus of the solitary tract and from the galaninergic RTN neurons that were not labeled with BDA. The galaninergic projection of RTN to the lateral parabrachial nucleus seemed to preferentially target the lateral crescent and central subnuclei (terminology after Fulwiler and Saper, 1984). The ventrolateral medullary projection areas encompassed all subdivisions of the respiratory column (caudal ventral respiratory group, rostral respiratory group, preBötzinger complex, and Bötzinger complex; terminology after Alheid et al., 2002) and extended to a minor degree into the A5 region. The projection was almost exclusively ipsilateral (not illustrated). The locus coeruleus and the midline raphe did not contain any galaninergic terminals from the BDA-labeled neurons.

The number of axonal varicosities that were both BDA and galanin-ir were counted in these three cases and their rostrocaudal distribution is shown in histogram form in Figure 4. Most of the identified varicosities (60.6 ± 6.8%) were located in the ventrolateral medulla, a very small proportion was detected within the NTS (5.8 ± 1.3%), and the balance (33 ± 8%) was

found in the dorsolateral pons (Kölliker-Fuse, intertrigeminal region, and dorsal lateral parabrachial region).

Innervation of the pre-Bötzinger complex by RTN-Phox2b neurons

The neurons of the pre-Bötzinger complex form the core of the respiratory rhythm generating circuitry and typically express very high levels of the neurokinin-1 receptor (NK1R) (Gray et al., 2001; Guyenet et al., 2002; Smith et al., 2009). We wished to determine whether RTN-Phox2b neurons contact this cell population.

In order to label RTN-Phox2b neurons, we injected a lentiviral vector that expresses the fusion protein channelrhodopsin2-mCherry selectively in Phox2b-expressing neurons (PRSx8-ChR2-mCherry) (Abbott et al., 2009b, c). With time, the fusion protein migrates throughout the neurons including their finest axonal branches; thus the viral vector can serve as an anterograde tracing tool. In the rostral ventrolateral medulla of the adult rat, Phox2b is expressed almost exclusively by a mixture of RTN and C1 adrenergic neurons. In order to minimize the number of transfected C1 neurons, PRSx8-ChR2-mCherry was injected into rats (n = 5) in which the rostral C1 neurons had been depleted by injecting a retrogradely transported catecholaminergic neuron-selective toxin into the thoracic spinal cord (saporin conjugated to an anti-dopamine hydroxylase antibody) (Schreihofer et al., 2000). As a result, in these rats (Fig. 5A), following injection of PRSx8-ChR2-mCherry lentivirus into the RTN region, mCherry was expressed predominantly by neurons devoid of TH immunoreactivity, i.e., by RTN-Phox2b neurons. The relative proportion (71 ± 4% RTN-Phox2b:C1 neurons) was estimated by counting the number of TH-positive or TH-negative mCherry-labeled somatic profiles that included a nucleus in a series of equidistant sections throughout the injection site.

Next, we determined whether the mCherry-labeled nerve terminals present in the region of the pre-Bötzinger complex originated from the RTN-Phox2b neurons or from the minority of transfected C1 neurons or from both cell types. In the pre-Bötzinger complex, almost none (0.2%) of the mCherry-labeled nerve terminals contained any detectable TH-immunoreactivity (n = 5 rats; 26,374 total terminals counted; Fig. 5C). To ascertain that this negative result was not a false-negative artifact, we inspected the raphe pallidus, which receives input from the C1 neurons but is probably not innervated by RTN-Phox2b neurons (Abbott et al., 2009c; Card et al., 2010). In this brain region, most of the mCherry-positive terminals were TH-ir (Fig. 5D). Thus, according to these results, the overwhelming majority of mCherry-labeled terminals present within the pre-Bötzinger complex originated from transfected RTN-Phox2b neurons.

Because RTN neurons contain VGLUT2 mRNA (Mulkey et al., 2004), we also examined whether their axonal varicosities within the pre-Bötzinger complex contain detectable levels of immunoreactive VGLUT2 protein. VGLUT2-mCherry co-localization was detected in 65% of the mCherry-positive varicosities (n = 3 rats, 4,246 boutons counted; Fig. 5E). We presume that one-third of what appeared to us as axonal varicosities may not be actual synapses. This interpretation could be tested by identifying actual synapses with a specific marker (e.g., synaptophysin).

Next, we examined whether the mCherry-positive terminals contacted the neurokinin-1 receptor (NK1R)-expressing neurons of the pre-Bötzinger complex by processing a series of sections from three animals for simultaneous detection of mCherry and NK1R immunoreactivity. Sections were examined under differential interference contrast optics at high magnification to search for close appositions between RTN terminals (nickel-intensified black DAB reaction) and the soma and dendrites of pre-Bötzinger complex neurons (light brown DAB reaction product). Close appositions between RTN terminals and

NK1R-imunoreactive somatodendritic profiles were commonly observed (example in Fig. 5F), including but not exclusively on medium-sized neurons with oval-shaped somata that expressed high levels of NK1R immunoreactivity and are suspected to be glutamatergic rhythmogenic neurons (preinspiratory/inspiratory, preI-I neurons (Guyenet and Wang, 2001).

Ultrastructure of RTN terminals in the pre-Bötzinger complex

The ultrastructure of the mCherry-ir RTN-Phox2b neuronal terminals located within the pre-Bötzinger complex was examined in three of the five rats described in the previous section. The mCherry-ir varicosities (n = 48) contained small clear vesicles and made synapses that were invariably asymmetric (Fig. 6A–D). All 48 synapses were located on dendrites.

DISCUSSION

To summarize the novel findings, galanin and VGLUT2 immunoreactivity are present in the axonal varicosities of RTN-Phox2b neurons, providing additional evidence that both substances are used as transmitters by these neurons. The galaninergic subset of RTN neurons has limited brainstem projections that are consistent with our previous general description of the RTN at large (Rosin et al., 2006; Abbott et al., 2009c). The projections are ipsilateral and restricted to the ventral respiratory column, the dorsolateral pons, and the ventrolateral portion of the caudal nucleus of the solitary tract (NTS). RTN-Phox2b neurons make numerous close appositions with a subset of pre-Bötzinger complex neurons suspected to play a central role in respiratory rhythm generation. These contacts have the ultrastructural features of excitatory glutamatergic synapses. We conclude that, regardless of the presence of galanin, RTN-Phox2b neurons are glutamatergic neurons and activate the breathing rate by a mechanism that includes monosynaptic excitation of pre-Bötzinger complex neurons.

Projections of the RTN Phox2b neurons

The galanin-based approach used in the present study tracks the projections of the RTN-Phox2b neurons very specifically because, within the region of the RTN, this peptide is not synthesized by any other type of neuron (Stornetta et al., 2009). The method has the advantage of completely excluding the projections from the C1 neurons, which is not possible when one uses a PRSx8-based lentivirus to track the projections of RTN-Phox2b neurons. The galanin method has one disadvantage, which is that it only traces the projections of a subset of RTN-Phox2b neurons (around 45%) (Stornetta et al., 2009). However, pending evidence to the contrary, this population seems representative of the RTN-Phox2b neurons because its electrophysiological properties are indistinguishable from those of the RTN neurons that do not express galanin (Stornetta et al., 2009; Guyenet et al., 2010b). Importantly, the galaninergic neurons are also presumably excitatory because they contain VGLUT2 mRNA like all RTN-Phox2b neurons (Stornetta et al., 2006, 2009). A second limitation of the study is that the BDA injections were targeted to the caudal end of the nucleus. The rostral portion of the RTN could therefore have additional projections that we did not detect.

The galaninergic RTN-Phox2b neurons traced in this study innervated a very small number of interconnected lower brainstem structures that have a well-characterized role in generating the respiratory outflow (Smith et al., 2009). These areas include the entire length of the ventral respiratory column from the Bötzinger region rostrally to the spinomedullary junction, the dorsolateral pons, and caudal regions of the NTS. The projection pattern of the galaninergic subset of RTN-Phox2b neurons agrees with our initial study based on the use of PRSx8 lentivirus in C1 neuron-depleted rats (Abbott et al., 2009c), which suggests that the

galaninergic subset of RTN Phox2b neurons innervates the same general central nervous system (CNS) regions as the rest of these neurons.

RTN-Phox2b neurons activate both the frequency of breathing and the intensity of the contraction of inspiratory and expiratory muscles (Abbott et al., 2009c; Marina et al., 2010; Kanbar et al., 2010). These various actions almost certainly require that the RTN-Phox2b neurons establish synapses with many components of the respiratory pattern generator (Smith et al., 2009) besides the pre-Bötzinger complex (Smith et al., 1991; Tan et al., 2008). Consistent with this view, the RTN-Phox2b neurons innervate the entire ventral respiratory column. The projections of the RTN galaninergic neurons to the NTS were sparse and confined to the region of the nucleus that processes respiratory-related information (Kubin et al., 2006; McCrimmon et al., 2008). The caudolateral NTS region contains bulbospinal inspiratory premotor neurons that could be the target of the RTN-Phox2b neurons.

The projections of the RTN-Phox2b neurons to the dorsolateral pons closely overlapped with the regions that project back to the ventral respiratory column, namely, the Kölliker-Fuse nucleus, the intertrigeminal region, and the lateral crescent of the lateral parabrachial complex (Chamberlin and Saper, 1992, 1998; Chamberlin, 2004). We had some difficulty distinguishing the “lateral crescent” from the central subnucleus of the lateral parabrachial complex as originally defined (Fulwiler and Saper, 1984). Chemical stimulation of this general region of the parabrachial complex (presumably central and lateral crescent nuclei) causes hyperpnea and raises blood pressure and heart rate (Chamberlin and Saper, 1992; Chamberlin, 2004; Boscan et al., 2005). Such responses are also typically elicited by stimulation of central chemoreceptors and could plausibly also be elicited by the excitatory input from the RTN-Phox2b neurons to the lateral parabrachial region.

The lateral crescent and neighboring lateral parabrachial subnuclei also receive input from the C1 neurons of the ventrolateral medulla and from neurons located within the superficial laminae of the spinal cord that relay nociceptive stimuli (Boscan et al., 2005; Card et al., 2006). This convergence of inputs suggests that the lateral crescent or a nearby parabrachial region could be contributing to the arousal or alerting responses caused by a variety of intero- or extero-nociceptive inputs that converge on this region, including hypoxia and hypercapnia (Phillipson et al., 1977; Bowes et al., 1981). The C1 neurons, activated by hypoxia, and the RTN-Phox2b neurons, activated by a rise in CNS PCO_2 and by hypoxia via the carotid bodies, could contribute such arousal-promoting inputs (Phillipson et al., 1977; Sun, 1996; Guyenet et al., 2010b). Patients with Phox2b mutations that presumably destroy the RTN-Phox2b neurons, experience severe sleep apnea that does not produce arousal (Weese-Mayer et al., 2010; Goridis and Brunet, 2010). The loss of the excitatory input from the RTN-Phox2b neurons to the parabrachial region may contribute to this arousal deficit.

RTN-Phox2b neurons are glutamatergic and excitatory

The presence of VGLUT2 mRNA in RTN neurons and the absence of detectable glutamic acid decarboxylase 67 (GAD67) and glycine transporter 2 (GlyT2) mRNA are currently the principal evidence that these neurons are glutamatergic (Mulkey et al., 2004). This hypothesis is also consistent with the fact that selective activation of RTN neurons increases breathing (Guyenet et al., 2010a). However, the respiratory network is replete with examples of mutually interacting inhibitory neurons that have the potential to stimulate breathing rate via disinhibition (Smith et al., 2009). The present study contributes two additional pieces of data in support of the notion that RTN neurons are functionally excitatory. First, the majority of the axonal varicosities of RTN neurons contain high levels of VGLUT2. This protein is necessary and sufficient for the exocytotic release of glutamate (Takamori et al., 2001). Second, the synapses that RTN-Phox2b neurons establish with other neurons within the pre-Bötzinger complex are distinctly asymmetric and therefore conform to the classic

morphology of excitatory glutamatergic synapses (Carlin et al., 1980). Incidentally, the fact that RTN-Phox2b neurons make bona fide synapses, although hardly unexpected, is in itself a novel observation. The respiratory stimulation elicited by moderately high frequency stimulation of RTN-Phox2b neurons has a very slow decay rate ($T_{1/2}$ > 10 s)(Abbott et al., 2009c), a characteristic that could suggest volume transmission (Olah et al., 2009; Okubo and Iino, 2011) or a slow form of metabotropic transmission. The present study does not exclude the possibility that RTN neurons operate partially by such mechanisms but it reveals that these neurons most likely also communicate via classic ionotropic synaptic transmission.

Do the C1 neurons project to the pre-Bötzinger complex?

After administration of PRSx8-ChR2-mCherry lentivirus into the RTN region of rats with DβH-saporin toxin lesions of C1, we found extremely few varicosities that contained both mCherry and TH immunoreactivity within the pre-Bötzinger complex, but such double-labeled terminals were common within the raphe pallidus. In these experiments, the bulbospinal C1 neurons were substantially depleted. Therefore, our results only indicate that the pre-Bötzinger complex did not receive input from the particular C1 cells that were transfected with the viral vector in these experiments. This was necessary for our ultrastrucural study to focus on the synaptic input from the RTN-Phox2b neurons. The ventrolateral medulla does receive projections from some of the C1 neurons (Card et al., 2006), and these projections could very well target the pre-Bötzinger complex because this network is activated by catecholamines (Doi and Ramirez, 2010).

RTN-Phox2b neurons target the pre-Bötzinger complex

Irrespective of whether or not they contain galanin, RTN-Phox2b neurons clearly target the pre-Bötzinger complex. The latter region contains neurons with an unusually high level of neurokinin-1 receptors (NK1Rs); these neurons are required for breathing (Gray et al., 2001). These NK1R-ir neurons have been shown previously to receive asymmetric (most likely excitatory) synapses from VGLUT2 terminals, although the origin of the VGLUT2 was not examined (Liu et al., 2003). NK1R was originally thought to be a specific marker of a population of excitatory neurons with commissural projections (pre-inspiratory/inspiratory[preI-I] neurons) that form the core of the respiratory rhythm-generating circuitry (Gray et al., 2001; Janczewski and Feldman, 2006; Smith et al., 2009). Further experimentation has confirmed that the neurons that express high levels of NK1R immunoreactivity are predominantly glutamatergic and also that preI-I neurons with commissural projections frequently express high levels of NK1R (Guyenet and Wang, 2001; Guyenet et al., 2002). However, the data also indicate that other types of pre-Bötzinger complex neurons, including glycinergic and perhaps some premotor neurons, also express this receptor (Guyenet and Wang, 2001; Hayes and Del Negro, 2007; Manzke et al., 2010). Nonetheless, based on the ability of the saporin-conjugated substance P analog to destroy neurons that express NK1R and immunohistochemical evidence, a relatively small proportion of the γ-aminobutyric acid (GABA)ergic and glycinergic neurons of the pre-Bötzinger complex seem to express the NK1R (Wang et al., 2003; Manzke et al., 2010).

Because NK1R immunoreactivity is not a diagnostic marker for the preI-I rhythmogenic neurons of the pre-Bötzinger complex, the present data do not prove that these particular cells receive an input from the RTN. However, this interpretation is highly probable given the vast number of close appositions between RTN-Phox2b neuronal terminals and NK1R-ir neurons that we observed in the region of the pre-Bötzinger complex. In any case, there are many reasons to suspect that RTN-Phox2b neurons do not only target the preI-I neurons. Effective regulation of the breathing rate probably requires co-activation of several types of neurons including the early-I neurons, which are inhibitory and also reside within the pre-

Bötzinger complex (Rubin et al., 2009). RTN neurons also regulate the tidal volume and probably do so in part by targeting inspiratory premotor neurons, as suggested by their dense innervation of the region of the ventral medulla that contains phrenic premotor neurons, the rostral ventral respiratory group (Alheid et al., 2002; Rybak et al., 2007; Abbott et al., 2009c).

Role of galanin

In the present study, galanin served only as a neuronal marker. Microinjection of galanin into the rostral ventrolateral medulla inhibits breathing without producing much change in blood pressure (Abbott et al., 2009a). There is currently no evidence that galanin released by the RTN-Phox2b neurons depresses respiration because selective stimulation of these neurons always activates breathing including in freely behaving rats (Abbott et al., 2009c; Kanbar et al., 2010). Inhibitory neuropeptides (e.g., enkephalins, somatostatin) are commonly synthesized by glutamatergic neurons in the ventrolateral medulla (Stornetta et al., 2003a, b). The physiological relevance of the short-term electrophysiological effects produced by injecting galanin and other neuropeptides into the brainstem is unclear.

Conclusions

The RTN-Phox2b neurons, including their galaninergic subset, selectively target the pontomedullary regions that generate breathing movements. These neurons are glutamatergic and excitatory, and form conventional asymmetric synapses, at least within the pre-Bötzinger complex. The RTN-Phox2b neurons make an important contribution to respiratory chemoreflexes and operate by targeting multiple components of the respiratory rhythm and pattern generator in addition to the pre-Bötzinger complex. The projections of the RTN-Phox2b neurons to the lateral parabrachial nucleus could conceivably contribute to the arousal caused by asphyxia.

Acknowledgments

Grant sponsor: National Institutes of Health; Grant numbers: HL74011 and HL28785 (to P.G.G.).

LITERATURE CITED

Abbott SB, Burke PG, Pilowsky PM. Galanin microinjection into the PreBötzinger or the Bötzinger complex terminates central inspiratory activity and reduces responses to hypoxia and hypercapnia in rat. Respir Physiol Neurobiol. 2009a; 167:299–306. [PubMed: 19527801]

Abbott SB, Stornetta RL, Socolovsky CS, West GH, Guyenet PG. Photostimulation of channelrhodopsin-2 expressing ventrolateral medullary neurons increases sympathetic nerve activity and blood pressure in rats. J Physiol. 2009b; 587:5613–5631. [PubMed: 19822543]

Abbott SBG, Stornetta RL, Fortuna MG, Depuy SD, West GH, Harris TE, Guyenet PG. Photostimulation of retrotrapezoid nucleus Phox2b-expressing neurons in vivo produces long-lasting activation of breathing in rats. J Neurosci. 2009c; 29:5806–5819. [PubMed: 19420248]

Alheid GF, Gray PA, Jiang MC, Feldman JL, McCrimmon DR. Parvalbumin in respiratory neurons of the ventrolateral medulla of the adult rat. J Neurocytol. 2002; 31:693–717. [PubMed: 14501208]

Boscan P, Dutschmann M, Herbert H, Paton JF. Neurokininergic mechanism within the lateral crescent nucleus of the parabrachial complex participates in the heart-rate response to nociception. J Neurosci. 2005; 25:1412–1420. [PubMed: 15703395]

Bowes G, Townsend ER, Kozar LF, Bromley SM, Phillipson EA. Effect of carotid body denervation on arousal response to hypoxia in sleeping dogs. J Appl Physiol. 1981; 51:40–45. [PubMed: 7263422]

Card JP, Sved JC, Craig B, Raizada M, Vazquez J, Sved AF. Efferent projections of rat rostroventrolateral medulla C1 catecholamine neurons: Implications for the central control of cardiovascular regulation. J Comp Neurol. 2006; 499:840–859. [PubMed: 17048222]

Card JP, Lois J, Sved AF. Distribution and phenotype of Phox2a-containing neurons in the adult Sprague-Dawley rat. J Comp Neurol. 2010; 518:2202–2220. [PubMed: 20437524]

Carlin RK, Grab DJ, Cohen RS, Siekevitz P. Isolation and characterization of postsynaptic densities from various brain regions: enrichment of different types of postsynaptic densities. J Cell Biol. 1980; 86:831–845. [PubMed: 7410481]

Chamberlin NL. Functional organization of the parabrachial complex and intertrigeminal region in the control of breathing. Respir Physiol Neurobiol. 2004; 143:115–125. [PubMed: 15519549]

Chamberlin NL, Saper CB. Topographic organization of cardiovascular responses to electrical and glutamate microstimulation of the parabrachial nucleus in the rat. J Comp Neurol. 1992; 326:245–262. [PubMed: 1362207]

Chamberlin NL, Saper CB. A brainstem network mediating apneic reflexes in the rat. J Neurosci. 1998; 18:6048–6056. [PubMed: 9671689]

Doi A, Ramirez JM. State-dependent interactions between excitatory neuromodulators in the neuronal control of breathing. J Neurosci. 2010; 30:8251–8262. [PubMed: 20554877]

Feldman JL, Mitchell GS, Nattie EE. Breathing: rhythmicity, plasticity, chemosensitivity. Annu Rev Neurosci. 2003; 26:239–266. [PubMed: 12598679]

Fulwiler CE, Saper CB. Subnuclear organization of the efferent connections of the parabrachial nucleus in the rat. Brain Res Rev. 1984; 7:229–259.

Goridis C, Brunet JF. Central chemoreception: lessons from mouse and human genetics. Respir Physiol Neurobiol. 2010; 173:312–321. [PubMed: 20307691]

Gourine AV, Kasymov V, Marina N, Tang F, Figueiredo MF, Lane S, Teschemacher AG, Spyer KM, Deisseroth K, Kas-parov S. Astrocytes control breathing rhrough pH-dependent release of ATP. Science. 2010; 329:571–575. [PubMed: 20647426]

Gray PA, Janczewski WA, Mellen N, McCrimmon DR, Feldman JL. Normal breathing requires preBötzinger complex neurokinin-1 receptor-expressing neurons. Nat Neurosci. 2001; 4:927–930. [PubMed: 11528424]

Guyenet PG, Wang H. Pre-Bötzinger neurons with pre-inspiratory discharges “in vivo” express NK1 receptors in the rat. J Neurophysiol. 2001; 86:438–446. [PubMed: 11431523]

Guyenet PG, Sevigny CP, Weston MC, Stornetta RL. Neurokinin-1 receptor-expressing cells of the ventral respiratory group are functionally heterogeneous and predominantly glutamatergic. J Neurosci. 2002; 22:3806–3816. [PubMed: 11978856]

Guyenet PG, Stornetta RL, Abbott SB, Depuy SD, Fortuna MG, Kanbar R. Central CO2-chemoreception and integrated neural mechanisms of cardiovascular and respiratory control. J Appl Physiol. 2010a; 108:995–1002. [PubMed: 20075262]

Guyenet PG, Stornetta RL, Bayliss DA. Central respiratory chemoreception. J Comp Neurol. 2010b; 518:3883–3906. [PubMed: 20737591]

Hayes JA, Del Negro CA. Neurokinin receptor-expressing pre-Botzinger complex neurons in neonatal mice studied in vitro. J Neurophysiol. 2007; 97:4215–4224. [PubMed: 17409172]

Hwang DY, Carlezon WA Jr, Isacson O, Kim KS. A high-efficiency synthetic promoter that drives transgene expression selectively in noradrenergic neurons. Hum Gene Ther. 2001; 12:1731–1740. [PubMed: 11560767]

Janczewski WA, Feldman JL. Distinct rhythm generators for inspiration and expiration in the juvenile rat. J Physiol. 2006; 570:407–420. [PubMed: 16293645]

Kanbar R, Stornetta RL, Cash DR, Lewis SJ, Guyenet PG. Photostimulation of Phox2b medullary neurons activates cardiorespiratory function in conscious rats. Am J Respir Crit Care Med. 2010; 182:1184–1194. [PubMed: 20622037]

Kang BJ, Chang DA, Mackay DD, West GH, Moreira TS, Takakura AC, Gwilt JM, Guyenet PG, Stornetta RL. Central nervous system distribution of the transcription factor Phox2b in the adult rat. J Comp Neurol. 2007; 503:627–641. [PubMed: 17559094]

Kubin L, Alheid GF, Zuperku EJ, McCrimmon DR. Central pathways of pulmonary and lower airway vagal afferents. J Appl Physiol. 2006; 101:618–627. [PubMed: 16645192]

Landry M, Bouali-Benazzouz R, Andre C, Shi TJ, Leger C, Nagy F, Hokfelt T. Galanin receptor 1 is expressed in a subpopulation of glutamatergic interneurons in the dorsal horn of the rat spinal cord. J Comp Neurol. 2006; 499:391–403. [PubMed: 16998907]

Liu YY, Wong-Riley MTT, Liu JP, Jia Y, Liu HL, Fujiyama F, Ju G. Relationship between two types of vesicular glutamate transporters and neurokinin-1 receptor-immunoreactive neurons in the pre-Bötzinger complex of rats: light and electron microscopic studies. Eur J Neurosci. 2003; 17:41–48. [PubMed: 12534967]

Manzke T, Niebert M, Koch UR, Caley A, Vogelgesang S, Hulsmann S, Ponimaskin E, Muller U, Smart TG, Harvey RJ, Richter DW. Serotonin receptor 1A-modulated phosphorylation of glycine receptor alpha3 controls breathing in mice. J Clin Invest. 2010; 120:4118–4128. [PubMed: 20978350]

Marina N, Abdala AP, Trapp S, Li A, Nattie EE, Hewinson J, Smith JC, Paton JF, Gourine AV. Essential role of Phox2b-expressing ventrolateral brainstem neurons in the chemosensory control of inspiration and expiration. J Neurosci. 2010; 30:12466–12473. [PubMed: 20844141]

McCrimmon DR, Mitchell GS, Alheid GF. Overview: the neurochemistry of respiratory control. Respir Physiol Neurobiol. 2008; 164:1–2. [PubMed: 18721910]

Mulkey DK, Stornetta RL, Weston MC, Simmons JR, Parker A, Bayliss DA, Guyenet PG. Respiratory control by ventral surface chemoreceptor neurons in rats. Nat Neurosci. 2004; 7:1360–1369. [PubMed: 15558061]

Nattie EE, Li A. Multiple central chemoreceptor sites: cell types and function in vivo. Adv Exp Med Biol. 2008; 605:343–347. [PubMed: 18085297]

Okubo Y, Iino M. Visualization of glutamate as a volume transmitter. J Physiol. 2011; 589:481–488. [PubMed: 21115644]

Olah S, Fule M, Komlosi G, Varga C, Baldi R, Barzo P, Tamas G. Regulation of cortical microcircuits by unitary GABA-mediated volume transmission. Nature. 2009; 461:1278–1281. [PubMed: 19865171]

Pattyn A, Morin X, Cremer H, Goridis C, Brunet JF. Expression and interactions of the two closely related homeobox genes Phox2a and Phox2b during neurogenesis. Development. 1997; 124:4065–4075. [PubMed: 9374403]

Paxinos, G.; Watson, C. The rat brain in stereotaxic coordinates. San Diego: Academic Press; 1998.

Phillipson EA, Kozar LF, Rebuck AS, Murphy E. Ventilatory and waking responses to CO2 in sleeping dogs. Am Rev Respir Dis. 1977; 115:251–259. [PubMed: 190927]

Ptak K, Burnet H, Blanchi B, Sieweke M, De Felipe C, Hunt SP, Monteau R, Hilaire G. The murine neurokinin NK_1 receptor gene contributes to the adult hypoxic facilitation of ventilation. Eur J Neurosci. 2002; 16:2245–2252. [PubMed: 12492418]

Rosin DL, Chang DA, Guyenet PG. Afferent and efferent connections of the rat retrotrapezoid nucleus. J Comp Neurol. 2006; 499:64–89. [PubMed: 16958085]

Rubin JE, Shevtsova NA, Ermentrout GB, Smith JC, Rybak IA. Multiple rhythmic states in a model of the respiratory central pattern generator. J Neurophysiol. 2009; 101:2146–2165. [PubMed: 19193773]

Rybak IA, Abdala AP, Markin SN, Paton JF, Smith JC. Spatial organization and state-dependent mechanisms for respiratory rhythm and pattern generation. Prog Brain Res. 2007; 165:201–220. [PubMed: 17925248]

Schreihofer AM, Stornetta RL, Guyenet PG. Regulation of sympathetic tone and arterial pressure by rostral ventrolateral medulla after depletion of C1 cells in rat. J Physiol. 2000:221–236. [PubMed: 11080264]

Smith JC, Ellenberger HH, Ballanyi K, Richter DW, Feldman JL. Pre-Bötzinger complex—a brainstem region that may generate respiratory rhythm in mammals. Science. 1991; 254:726–729. [PubMed: 1683005]

Smith JC, Abdala AP, Rybak IA, Paton JF. Structural and functional architecture of respiratory networks in the mammalian brainstem. Philos Trans R Soc Lond B Biol Sci. 2009; 364:2577–2587. [PubMed: 19651658]

Stornetta RL, Rosin DL, Wang H, Sevigny CP, Weston MC, Guyenet PG. A group of glutamatergic interneurons expressing high levels of both neurokinin-1 receptors and somatostatin identifies the region of the pre-Bötzinger complex. J Comp Neurol. 2003a; 455:499–512. [PubMed: 12508323]

Stornetta RL, Sevigny CP, Guyenet PG. Inspiratory augmenting bulbospinal neurons express both glutamatergic and enkephalinergic phenotypes. J Comp Neurol. 2003b; 455:113–124. [PubMed: 12455000]

Stornetta RL, Moreira TS, Takakura AC, Kang BJ, Chang DA, West GH, Brunet JF, Mulkey DK, Bayliss DA, Guyenet PG. Expression of Phox2b by brainstem neurons involved in chemosensory integration in the adult rat. J Neurosci. 2006; 26:10305–10314. [PubMed: 17021186]

Stornetta RL, Spirovski D, Moreira TS, Takakura AC, West GH, Gwilt JM, Pilowsky PM, Guyenet PG. Galanin is a selective marker of the retrotrapezoid nucleus in rats. J Comp Neurol. 2009; 512:373–383. [PubMed: 19006184]

Sun MK. Pharmacology of reticulospinal vasomotor neurons in cardiovascular regulation. Pharmacol Rev. 1996; 48:465–494. [PubMed: 8981563]

Takakura AC, Moreira TS, Stornetta RL, West GH, Gwilt JM, Guyenet PG. Selective lesion of retrotrapezoid Phox2b-expressing neurons raises the apnoeic threshold in rats. J Physiol. 2008; 586:2975–2991. [PubMed: 18440993]

Takamori S, Rhee JS, Rosenmund C, Jahn R. Identification of differentiation-associated brain-specific phosphate transporter as a second vesicular glutamate transporter (VGLUT2). J Neurosci. 2001; 21:NIL7–NIL12.

Tan W, Janczewski WA, Yang P, Shao XM, Callaway EM, Feldman JL. Silencing preBötzinger complex somatostatin-expressing neurons induces persistent apnea in awake rat. Nat Neurosci. 2008; 11:538–540. [PubMed: 18391943]

Wang H, Weston MC, McQuiston TJ, Stornetta RL, Guyenet PG. Neurokinin-1 receptor-expressing cells regulate depressor region of rat ventrolateral medulla. Am J Physiol Heart Circ Physiol. 2003; 285:H2757–H2769. [PubMed: 12933345]

Weese-Mayer DE, Berry-Kravis EM, Ceccherini I, Keens TG, Loghmanee DA, Trang H. An official ATS clinical policy statement: congenital central hypoventilation syndrome: genetic basis, diagnosis, and management. Am J Respir Crit Care Med. 2010; 181:626–644. [PubMed: 20208042]

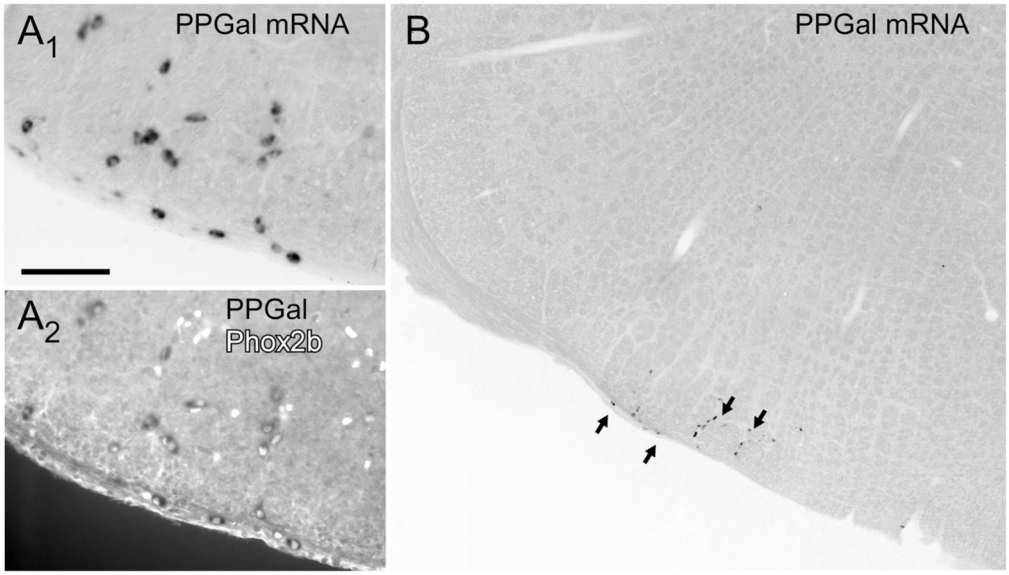

Figure 1.

Preprogalanin (PPGal) mRNA in the retrotrapezoid nucleus. **A1**: PPGal mRNA-containing neurons (brightfield illumination) with mRNA revealed by nonradioactive digoxigenin immunohistochemistry using alkaline phosphatase and nitroblue tetrazolium/5-bromo-4-chloro-3-indolyl-phosphate as substrate (see Stornetta et al., 2009 for details). **A2**: Same field photographed under fluorescent light to reveal the Phox2b-immnoreactive (ir) nuclei. Every PPGal-mRNA-positive neuron contains a Phox2b-ir nucleus. **B**: Photomontage illustrating the isolation of the cluster of PPGal-mRNA-positive retrotrapezoid nucleus (RTN) neurons. Scale bar in A1 = 100 μm for A1, A2; 330 μm for B.

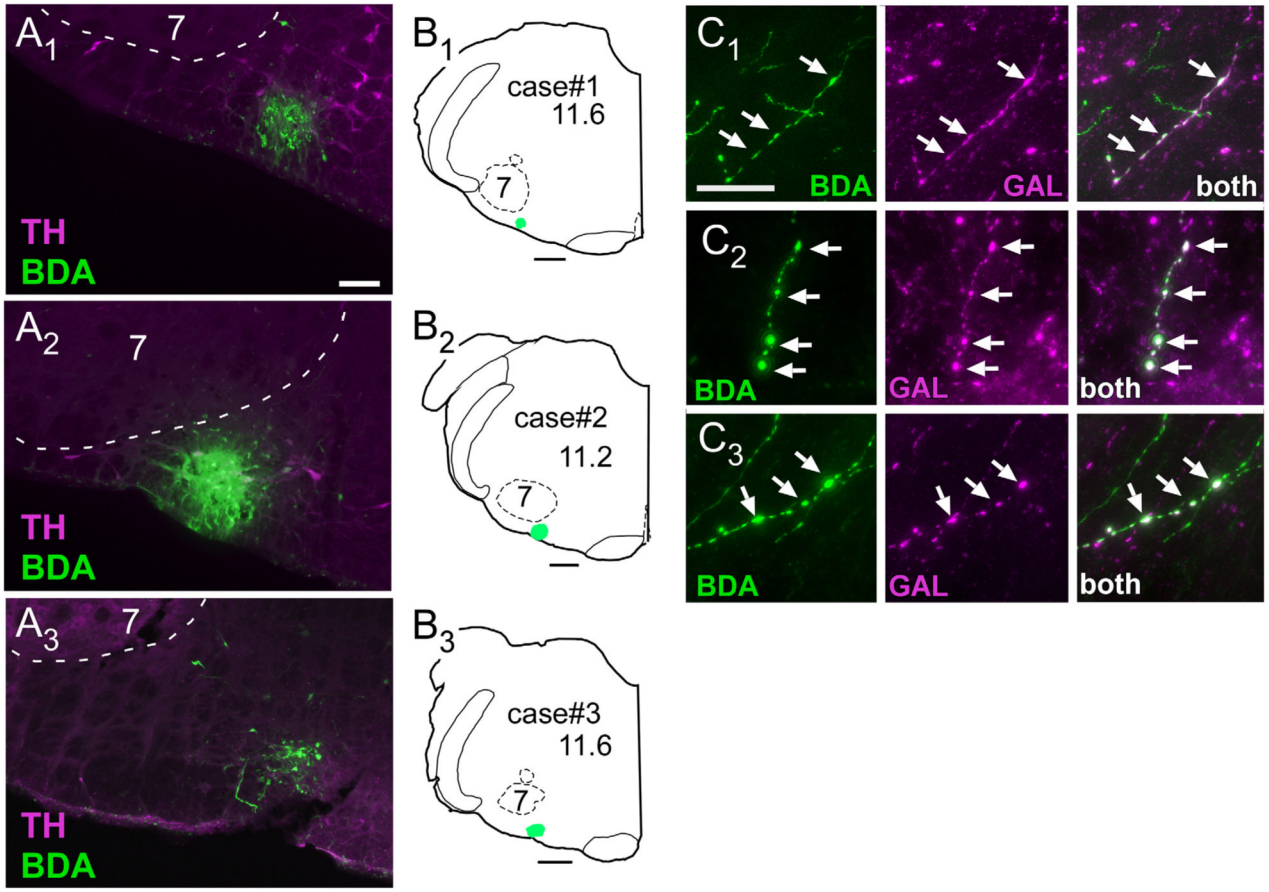

Figure 2.

BDA injection sites and anterograde labeling of galaninergic axonal processes. **A1–A3**: Injection sites of biotinylated dextran amine (BDA) in three rats. The iontophoretic injections of BDA (revealed with Alexa-488, green fluorescence) were deliberately targeted below the caudal edge of the facial motor nucleus where the highest density of RTN Phox2b neurons reside. This region sits at the lateral edge of the column of C1 adrenergic neurons (identified by immunohistochemical detection of tyrosine-hydroxylase [TH] with Cy-3, in magenta). **B1–B3**: Computer-generated drawings of the location in coronal sections of the three BDA injection sites shown in A. The numbers below the case numbers refer to mm behind bregma after the atlas of Paxinos and Watson (1998). **C1–C3**: Examples of galanin-ir terminals (shown in magenta) containing BDA (BDA alone is green, double-labeled terminals appear white) within the pre-Bötzinger complex (C1), Kölliker-Fuse nucleus (C2), and lateral parabrachial nucleus (C3). Scale bar = 100 μm in A1 (applies to A1–A3); 500 μm in B1–B3; 10 μm in C1 (applies to C1–C3).

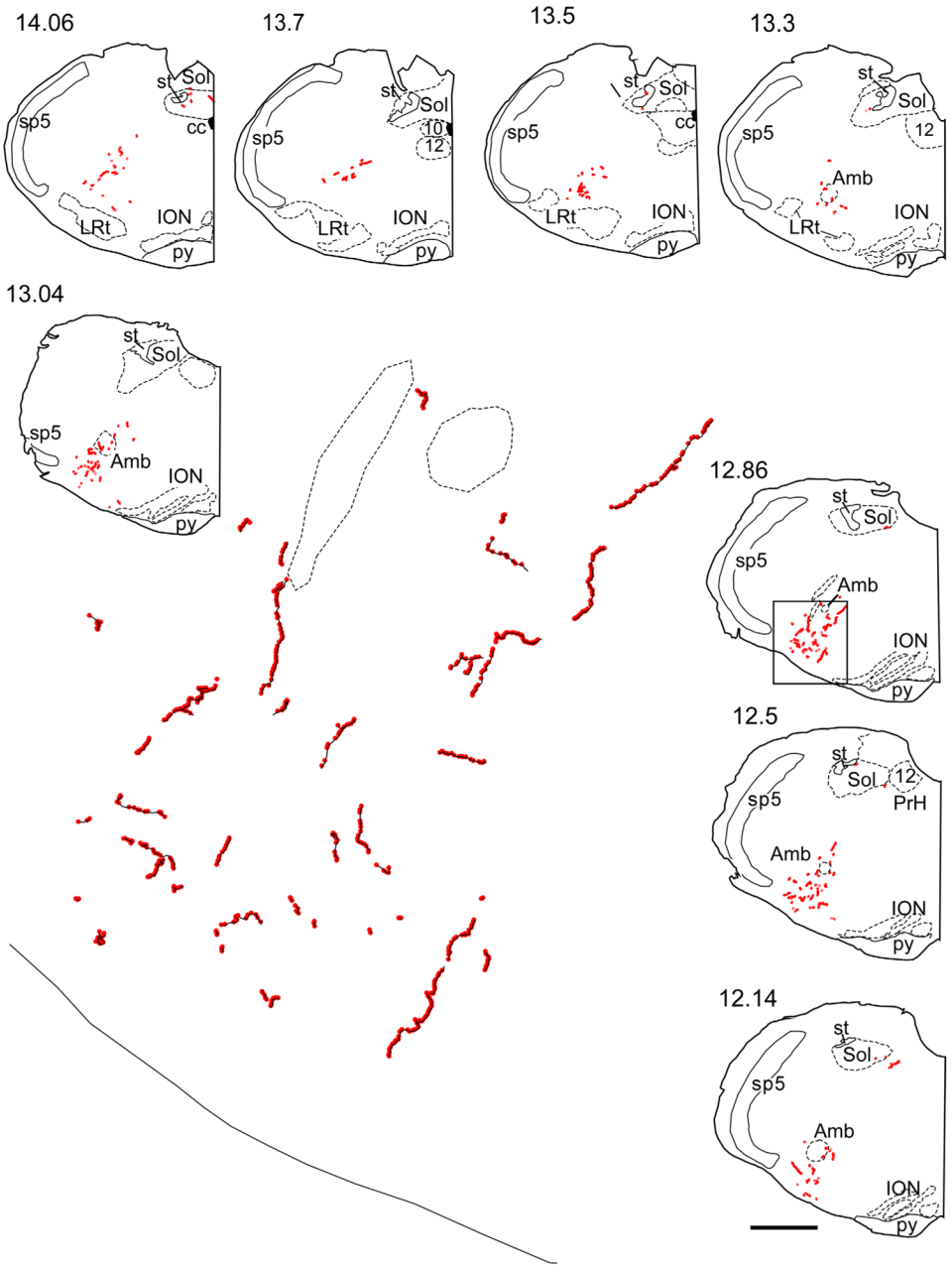

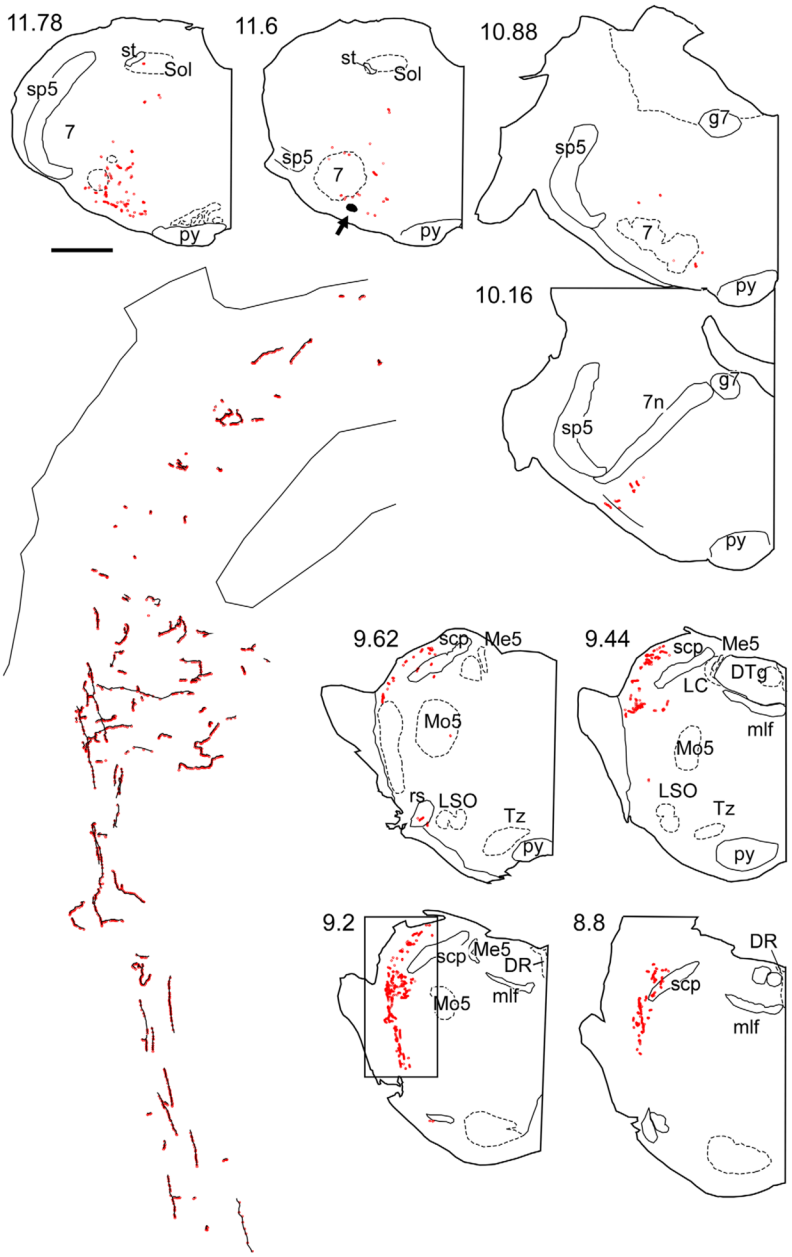

Figure 3.

Representative example of CNS projections of the retrotrapezoid galaninergic neurons. The axonal varicosities that were immunoreactive for BDA and galanin are selectively represented as red dots on these computer-assisted drawings of coronal hemisections. The numbers to the upper left of each coronal hemisection drawing indicate the location of the section as the approximate number of mm caudal to bregma after the atlas of Paxinos and Watson (1998). The area in the rectangular box in section 12.86 corresponds to the pre-Bötzinger complex, and an enlargement showing fibers in black and boutons in red is shown in the middle. In the continuation panel, the area in the rectangular box in section 9.2 corresponds to the lateral parabrachial nucleus/Kölliker Fuse area, and an enlargement showing fibers in black and boutons in red is shown on the left side on the continuation panel. The arrow at level 11.6 mm caudal to Bregma points to the BDA injection site.

Abbreviations: 7, facial nucleus; 12, hypoglossal nucleus; 7n, facial nucleus root; Amb, ambiguus nucleus; cc, central canal; DR, dorsal raphe nucleus; DTg, dorsal tegmental nucleus; g7, genu of facial nucleus; ION, inferior olivary nucleus; LRt, lateral reticular nucleus; LSO, lateral superior olive; Me5, mesencephalic 5 nucleus; mlf, medial longitudinal fasciculus; Mo5, motor trigeminal nucleus; py, pyramidal tract; rs, rubrospinal tract; scp, superior cerebellar peduncle; Sol, nucleus of the solitary tract; Sp5, spinal trigeminal nucleus; st, solitary tract; Tz, nucleus of trapezoid body. Scale bar = 1 mm for all smaller drawings, 0.09 mm for the enlargement representing the pre-Bötzinger complex, and 0.154 mm for the enlargement representing the parabrachial/Kölliker Fuse area. [Color figure can be viewed in the online issue, which is available at wileyonlinelibrary.com.]

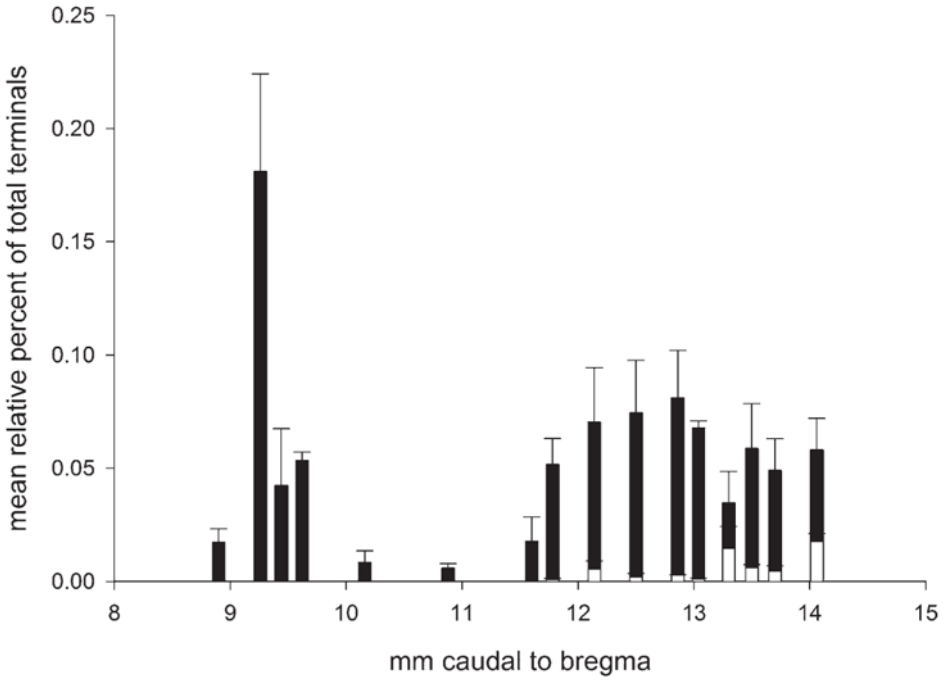

Figure 4.

Rostrocaudal distribution of boutons containing BDA and galanin immunoreactivity. Frequency distribution histogram of double-labeled boutons based on the three BDA cases shown in Figure 2. The boutons located at levels between 8 and 10 mm behind bregma were all within the dorsolateral pons (closed bars). The boutons located caudal to the region at 11 mm behind bregma were in two regions (ventrolateral medulla and nucleus of the solitary tract) and are represented separately (closed and open bars, respectively).

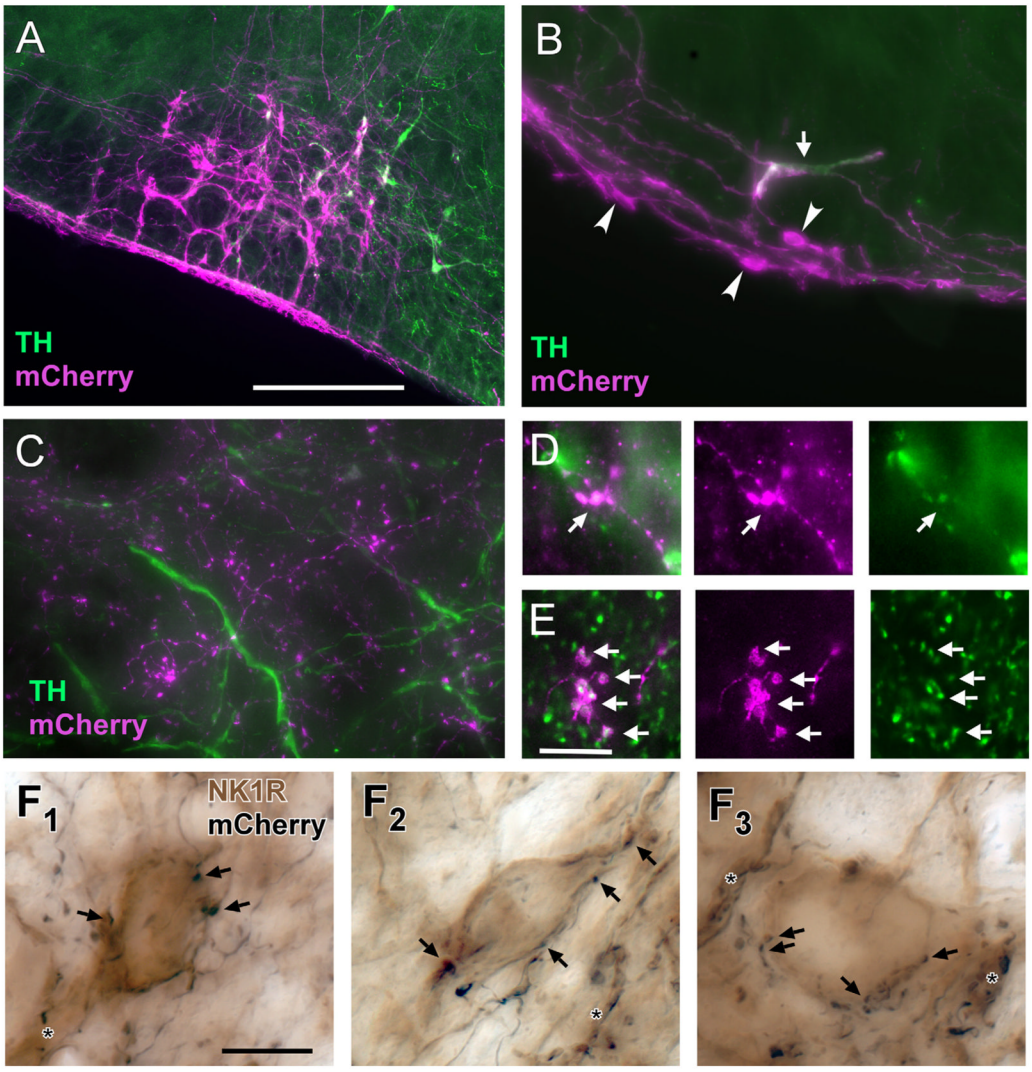

Figure 5.

Terminals of RTN-Phox2b neurons make close appositions with NK1R-ir neurons in the pre-Bötzinger complex. **A**: Example of mCherry-ir neurons within the RTN region 3 weeks after injection of PRSX8 ChR2-mCherry lentivirus into rats pretreated with anti-DβH-saporin to reduce the number of spinally projecting TH neurons. The vast majority of the transfected neurons are not TH-ir (TH immunofluorescence in green; ChR2-expressing TH neurons in white). **B**: Higher magnification example showing a single TH-ir neuron (arrow) and multiple TH-negative neurons (arrowheads) that contain mCherry (magenta). The depicted region is below the facial motor nucleus. The TH-negative neurons are located within the marginal layer of the RTN. **C**: The mCherry-ir terminals (magenta) located within the pre-Bötzinger complex do not contain TH immunoreactivity (green). **D**: mCherry-ir terminals (magenta) located within the raphe pallidus are TH-ir (TH in green, double-labeled terminals appear white). **E**: A large fraction of the mCherry-ir (magenta) terminals located within the Pre-Bötzinger complex are positive for VGLUT2 (green, double-labeled terminals appear white). **F1–F3**: Examples of close appositions between mCherry-ir varicosities (nickel-enhanced DAB reaction, black) and NK1R-ir somata or dendrites within the pre-Bötzinger complex (light brown). Some of the close appositions (putative synapses) are indicated by arrows. Close appositions on dendrites are indicated by the asterisks. Scale

bar = 250 μm in A (applies to A–C); 10 μm in E (applies to D, E); 10 μm in F1 (applies to F1–F3).

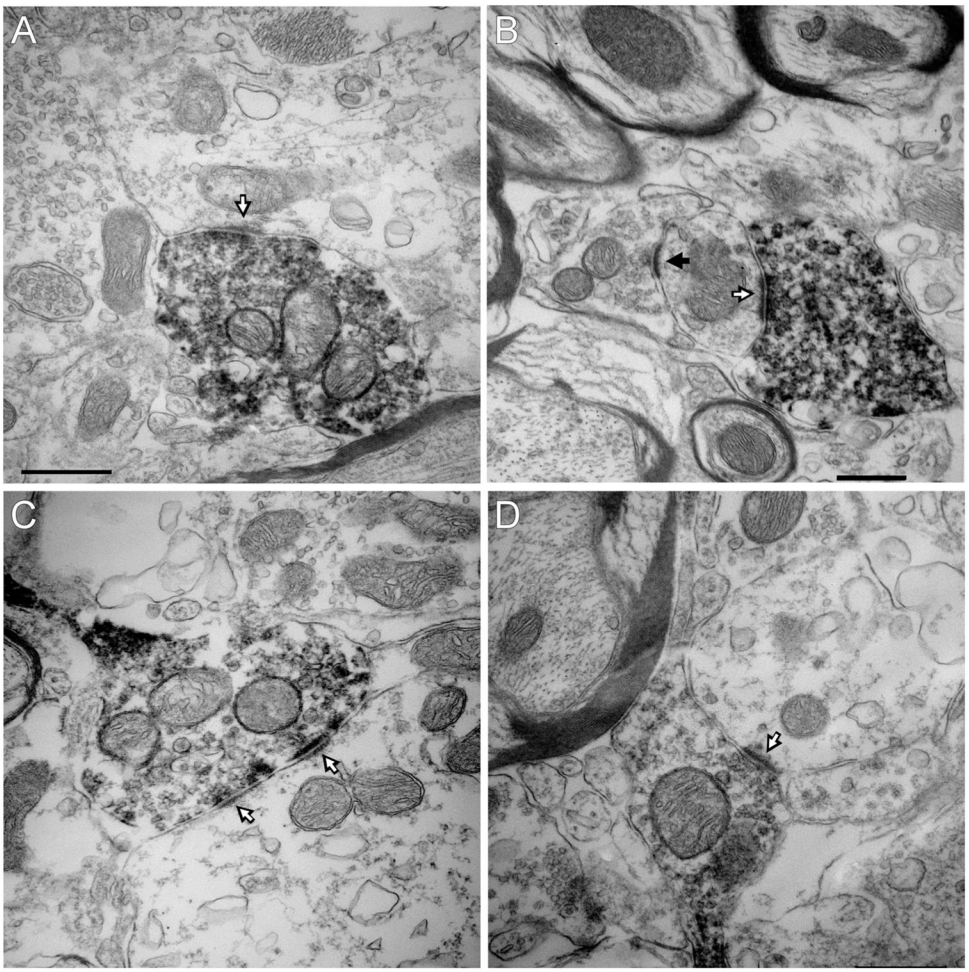

Figure 6.

Ultrastructure of the synaptic contacts between RTN-Phox2b neurons and pre-Bötzinger complex neurons. **A–D**: The mCherry-ir terminals of the RTN-Phox2b neurons contain intracellular and plasma membrane-associated electron-dense immunoperoxidase reaction product. These terminals make asymmetric synaptic contacts with unlabeled dendrites. The white arrows identify the thick postsynaptic material characteristic of excitatory glutamatergic synapses. The black arrow points to an asymmetric contact between an unlabeled terminal and a dendrite. Scale bar = 0.5 μm in A (applies to A, C, D); 0.5 μm in B.